Journal of Cleaner Production 286 (2021) 125294

Contents lists available at ScienceDirect

Journal of Cleaner Production

journal homepage: www.elsevier.com/locate/jclepro

Life cycle inventory of samarium-cobalt permanent magnets, compared to neodymium-iron-boron as used in electric vehicles

Gwendolyn Bailey [a, *], Martina Orefice [b], Benjamin Sprecher [c], Mehmet Ali Recai Önal [b], Enrique Herraiz [d], Wim Dewulf [e], Karel Van Acker [f]

[a] KU Leuven, Department of Materials Engineering, Kasteelpark Arenberg 44, 3001, Leuven, Belgium
[b] KU Leuven, Department of Chemistry, Celestijnenlaan 200, 3001, Leuven, Belgium
[c] Leiden University, Institute of Environmental Sciences (CML), Einsteinweg 2, 2333 CC, Leiden, the Netherlands
[d] University of Birmingham, School of Metallurgy and Materials, Edgbaston, Birmingham, B15 2TT, United Kingdom
[e] KU Leuven, Department of Mechanical Engineering, Celestijnenlaan 300, 3001, Leuven, Belgium
[f] KU Leuven, Department of Materials Engineering and Research Centre for Economics and Corporate Sustainability, Kasteelpark Arenberg 44, 3001, Leuven, Belgium

ARTICLE INFO

Article history:
Received 19 August 2019
Received in revised form
15 October 2020
Accepted 24 November 2020
Available online 8 December 2020

Handling editor: Yutao Wang

Keywords:
Cobalt
Electric motors
Life cycle inventory
Rare earth elements
Permanent magnets
Life cycle assessment

ABSTRACT

Electric vehicles are sometimes marketed unambiguously as low-carbon technologies; however, they often contain less 'clean' ingredients, such as rare earth permanent magnets. In fact, high-performance permanent magnets in electric vehicles often use neodymium. Alternatively, more costly samarium-cobalt magnets can be used. In this paper, life cycle assessment is used to compare the primary production routes of both neodymium-iron-boron and samarium-cobalt magnets in terms of environmental impact. For primary production of samarium-cobalt magnets, this is the first detailed life cycle inventory published to date. In addition, we provide an updated life cycle assessment of neodymium-iron-boron, expanded with recent literature and some primary industry data.

We conclude that production of samarium-cobalt is not preferable in terms of environmental impact, from a cradle-to-gate perspective. A sensitivity analysis and uncertainty analysis show that while there are uncertain parameters in both studies, the uncertainty range tends to be slightly higher for samarium-cobalt.

1. Introduction

Paradoxically, the materials used in the low carbon technologies of the future are often sourced in an environmentally-damaging and carbon-intense way: permanent magnet (PM) production is not different. The advancement of PMs is driven by the miniaturization of magnetic material coupled with increased property performance. The environmental damage associated with the production of these magnets is of increasing concern both to policy makers and industry. As such, the choice of magnetic alloy should be further considered in terms of product design for PMs in electric motors.

Prior to the 1980s, the best temperature-resistant and energy-dense magnets available were samarium-cobalt (SmCo) based, and could be found in a majority of PM applications (Strnat et al., 1967). However, the Japanese company Sumitomo and the American company General Motors wanted to develop a magnet with good performance at a lower cost (Krishnamurthy and Gupta, 2005). Thus the neodymium-iron-boron (NdFeB) magnet was developed (Herbst et al., 1984; Sagawa et al., 1985). The rapid transition from SmCo to NdFeB was partly due to problems with the supply of cobalt. Civil unrest (in 1978) in the Democratic Republic of Congo, formerly Zaire, threatened about half the world's supply of refined cobalt metal. At that time, NdFeB was found to be an appropriate substitute for SmCo as it was both cheaper, less subject to price volatility, and supply was not deemed at risk. Since then, NdFeB PMs have been the standard choice of PM used in most

* Corresponding author.
E-mail addresses: gwensusername@gmail.com (G. Bailey), Martina.Orefice@kuleuven.be (M. Orefice), Sprecher@cml.leidenuniv.nl (B. Sprecher), mehmetalirecai.onal@kuleuven.be (M.A.R. Önal), enriqueherraizlalana@gmail.com (E. Herraiz), Wim.Dewulf@kuleuven.be (W. Dewulf), Karel.Vanacker@kuleuven.be (K. Van Acker).

https://doi.org/10.1016/j.jclepro.2020.125294
0959-6526/

electronic applications such as hard disk drives, cell phones, and electric vehicle motor/generators.

Nevertheless, SmCo PMs do retain some advantages over NdFeB PMs. These include better corrosion resistance and greater magnetic output at temperatures above 150 °C circa. The elevated temperatures of a vehicle drive train require magnets with superior coercivity. Adding dysprosium or terbium could improve NdFeB magnets' Curie temperature and the performance at higher temperature (Chen et al., 2015). Unfortunately, both dysprosium and terbium are heavy rare earth elements (HREE) with relatively low reserves bases and both are significantly more expensive than neodymium. In some cases, this makes the use of SmCo magnets more cost-effective (Magenti Ljubljana, 2013). Despite these advantageous properties, the market share of SmCo for PMs is around 2% (Binnemans et al., 2013). It should be noted that changing the chemical compositions of the magnets will affect the chemical and thermal stability and the magnetic strength could be jeopardized. There are multiple formulations of SmCo: we only focus on 1:5 because that is the one focused on in the European Training Network DEMETER project. In this work, SmCo refers to $SmCo_5$, unless explicitly stated otherwise. Note that using different magnet types may also affect the design of the motors, thus indirectly affect the environmental footprints. This aspect is not considered in the current study.

While several life cycle assessment (LCA) studies have been performed for NdFeB magnets (Marx et al., 2018; Sprecher et al., 2014), and other oxide forms of rare earth elements (REEs) (Navarro and Zhao, 2014; Schreiber et al., 2016; Tharumarajah and Koltun, 2011; Vahidi, Navarro and Zhao, 2016), we are not aware of any fully detailed, process-specific SmCo magnet LCA studies. The LCA works related to NdFeB magnets are either modeled using black box data from an LCA data service or are modeled using a process-specific life cycle inventory (LCI). There have been many more efforts to elaborate on NdFeB data as opposed to SmCo data, due to the former being the more common magnet material of choice in e-motors. In this work, we answer the question: will the substitution of NdFeB-based PMs by SmCo-based PMs reduce environmental impact?

2. Methodology

LCA methodology was used to compare the environmental impact of producing 2.04 kg of $SmCo_5$ magnet with 1 kg of NdFeB magnet, in accordance with (Guinée and Lindeijer, 2002). The LCI was constructed using the software package GaBi (version 8.5). The LCI is the aggregated sum of each of the environmental exchanges. Simply put, this is a list of calculations of resources extracted from and emissions released to the environment. The resource and emission exchanges in the LCI can then be characterized according to their impact on the environment. Characterization factors are based on widely reviewed natural science-based models and are described in the impact assessment method. To enable comparison with the previous study by Sprecher et al. (2014) the CML2001 – 2013 impact assessment method was used. Section 2.1 contains the goal and scope of this study. Section 2.2 describes the LCIs for the production of NdFeB and SmCo. The full LCIs for both processes are provided in the Supporting Information.

2.1. Goal and scope

The methodological decisions made in order to define the LCA are referred to as the scope of the LCA. The system boundaries of the present study include the entire production chain of both NdFeB and SmCo PMs, from mining to the production of the magnet. We do not consider the use and end-of-life (EoL) phases. See Scheme 1 for a schematic representation. The setting of system boundaries serves to both help and hinder the study. It is advantageous in that it allows for a highly detailed mapping of the environmental impacts during the production of the magnets; however, it limits the results in that we cannot determine the environmental impact of the product in the wider context of its end application.

As a functional unit, we use the energy density and functionality of 1.0 kg of NdFeB. This corresponds to 2.04 kg of SmCo, based on

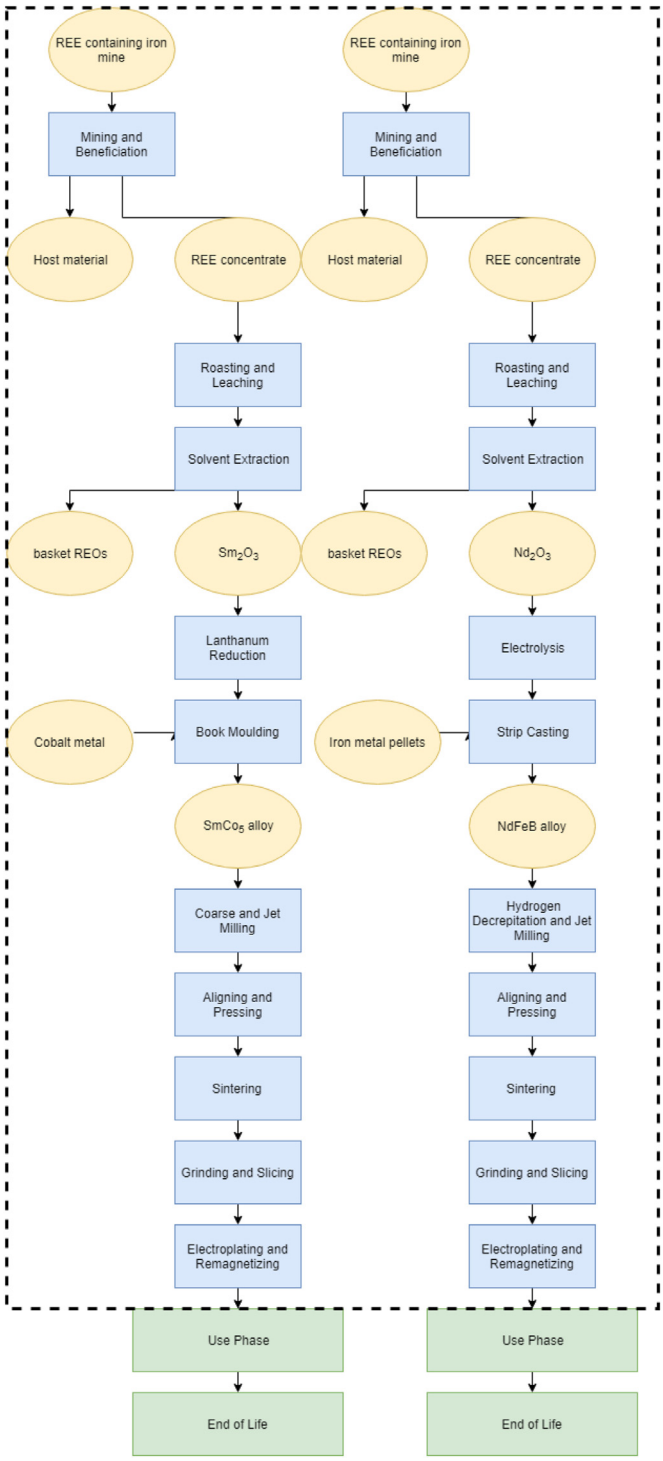

Scheme 1. Processing, from cradle-to-gate, flowsheet differences between SmCo (left) and NdFeB (right).

the magnetic energy density per unit volume, referred to as the maximum energy product or $(BH)_{max}$. See Table 1 for conversion parameters.

2.2. Life cycle inventory of NdFeB and $SmCo_5$ production

Although the production processes of NdFeB and SmCo differ significantly, parts of the REE production and final stages of magnet production overlap, as seen in Scheme 1. For REE production, the processes differ after solvent extraction (SX). Magnet production differs until it converges at jet milling. We first discuss the LCI of NdFeB in section 2.2.1, followed by a description of the LCI of SmCo in section 2.2.2.

2.2.1. NdFeB life cycle inventory

The NdFeB LCI is based on Sprecher et al. (2014), updated to include the latest data available. First, all background processes were updated to Ecoinvent version 3.3 (Wernet et al., 2016); second, the proxy used for 'organic chemicals' was updated with recent data on solvents from Vahidi and Zhao (2017). Third, several values in the beneficiation and SX processes were updated according to Lee and Wen (2017). Finally, rare earth oxide (REO) values were updated to reflect the average prices of the past 10 years. The latter led to a shift in allocation in the SX process, because REO prices decreased from Sprechers' original figures (from 85 USD per kg of Nd_2O_3 to 45 USD per kg). Finally, we note that for electroplating of NdFeB, it was not possible to obtain values for wastewater. This could yield significant effects since 1 m^3 of wastewater treatment for black chrome nickel plating results in a Global Warming Potential (GWP) impact of 0.2 kg of CO_2 per kg of NdFeB magnet.

A complete overview of the final data used in this study for each process can be found in the Supporting Information – NdFeB LCI, where changes from Sprecher et al. (2014) are highlighted in red.

2.2.2. SmCo life cycle inventory

Due to the lack of LCI data within the rare earth industry Bailey et al. (2020), our SmCo LCI data are based on a mixture of literature sources, industry data, interviews with experts, and Ecoinvent background data (Table 2). An overview of the SmCo production process and modeling choices is given in the following subsections. A detailed discussion of the assumptions together with the full LCI data can be found in the Supporting Information – SmCo LCI.

2.2.2.1. Cobalt mining and production route. Cobalt production is based on the LCI dataset provided by the Cobalt Development Institute (CDI), which is based on primary data coming from eight cobalt producers, representing 30% of total global production. As such, it is currently the most comprehensively available LCI data on cobalt (The Cobalt Development Institute, 2016). The dataset covers the production of cobalt (metal and powder) obtained as a co-product from mining/production of both nickel and copper, and applies a combination of mass allocation and economic allocation, since cobalt attracts a higher price than its main co-products (The Cobalt Development Institute, 2016) (Santero and Hendry, 2016).

2.2.2.2. Samarium mining and beneficiation. The mining and beneficiation of samarium follows a similar route to that of neodymium as described in Sprecher et al. (2014), with values being adjusted to account for the main product being samarium rather than neodymium (i.e. the total ore required to produce the functional unit).

Many types of ore contain samarium, with bastnaesite being the most common one (Li and Yang, 2014). Although bastnaesite is not the richest in samarium, its rich overall REEs content and simple composition make it the most convenient to process for the production of all REEs, in particular of the light ones, such as samarium (Shi, 2009). Sprecher et al. (2014) also considered bastnaesite as the source of neodymium and samarium. The largest site of bastnaesite is Bayan Obo in Inner Mongolia but not all samarium is produced from bastnaesite. Although environmental and energy data for this mine are largely kept confidential due to commercial sensitivity, recent studies provide information on Chinese specific emissions from Chinese standards, but it is not necessarily specific to any facility (Chinese Ministry of Environmental Protection, 2011; Lee and Wen, 2017). The mining process in Bayan Obo is both physically and chemically similar to iron ore mining. Environmental inflows and outflows of the process are therefore assumed to be the same, except for the difference in ore concentration which has been calculated (Li and Yang, 2014). The model for the beneficiation process includes the combination of chemicals and energy used for removal from REEs concentrate from a tailings stream containing predominantly Fe_2O_3. Ores are initially crushed to the desired particle size. A series of weak and then strong magnetic separation removes iron from the ore to be processed separately. The last step is froth flotation, where fatty acid collectors are added which adhere to the bastnaesite. This causes them to float to the surface of the solution where they can be captured.

2.2.2.3. Acid roasting and leaching. The acid roasting process is based on Sprecher et al. (2014), see Supporting Information – SmCo LCI for more detailed information.

At the Bayan Obo mining site, the mineral concentrate from beneficiation is roasted with sulfuric acid and then leached. Sulfuric acid is a common reactant to dissolve mixed concentrates containing carbonatite minerals. Such high-temperature acid-roasting process is relatively simple but generates potentially hazardous exhaust gases such as hydrogen fluoride (HF). These hazardous products can be removed by scrubbing before releasing the gas into the environment. However, this is not known to be a common practice in China. The main reaction is given in equation (1):

$$Sm_2O_3 + 3H_2SO_4 = Sm_2(SO_4)_3 + 3H_2O \quad (1)$$

The radioactive elements present in the ore react with the sulfuric acid, as given in equations (2) and (3):

$$ThO_2 + 2\ H_2SO_4 \rightarrow Th(SO_4)_2 + 2\ H_2O \quad (2)$$

$$2\ U_3O_8 + O_2 + 6\ H_2SO_4 \rightarrow 6\ UO_2SO_4 + 6\ H_2O \quad (3)$$

The content of ThO_2 and U_3O_8 in the ore are, respectively,

Table 1
Conversion of magnets maximum energy product into energy per kg.

	Magnetic energy density kJ/m^3	Density kg/m^3	Magnetic energy per unit mass kJ/kg	Relative magnetic energy per unit mass –
NdFeB	450	7625	0.059	1 (reference)
SmCo	240	8300	0.029	2.04

Table 2
LCI (foreground and background) sources for SmCo LCA.

Production Stage	References
Mining	(Sprecher et al., 2014), Ecoinvent, Thinkstep, (IEA, 2011) (Norgate and Haque, 2010),(The Cobalt Development Institute, 2016)
Beneficiation	(Peiró and Méndez, 2013), Ecoinvent, Thinkstep, (Sprecher et al., 2014),(Lee and Wen, 2017), (IEA, 2011)
Acid Roasting	(Sprecher et al., 2014), Ecoinvent, own calculations
Leaching	(Sprecher et al., 2014), Ecoinvent, own calculations
Solvent Extraction	Ecoinvent, (Lee and Wen, 2017), Calculations, (Sprecher et al., 2014)
Lanthanum Reduction	(Lee and Wen, 2017), (Ministry of Environmental Protection, 2009), Thinkstep, (Krishnamurthy and Gupta, 2005)
Book Molding	Ecoinvent, Industrial source, (The Cobalt Development Institute, 2016)
Coarse Milling	Ecoinvent, Industrial source
Jet Milling	(Sprecher et al., 2014), Industrial source, Ecoinvent
Aligning and Pressing	Industrial source
Sintering	Industrial source, (Sprecher et al., 2014), Ecoinvent
Grinding and Slicing	Ecoinvent, Industrial source
Electroplating	Ecoinvent, (Moign et al., 2009), (Sprecher et al., 2014), Industrial source

<0.3 wt% and <0.1 wt%, and are calculated based on the proportion of a samarium content equal to 0.8 wt% (Jordens et al., 2013) (IEA, 2011). In equation (3), the consumption of O_2 from air is negligible in terms of quantity. The total consumption of H_2SO_4 is not stoichiometric. In fact, a mass ratio acid/mineral between 1:1 and 2:1 is used to face the consumption of acid by the high content of carbonates and iron in the gangue. To be conservative, the present study uses an average ratio of 1.7. The results are listed in Table 3.

After that, the $REE_2(SO_4)_3$ is converted into a $REECl_3$ in a leaching step. This is carried out according to the reaction:

$$REE_2(SO_4)_3 + 6\,HCl + 3\,Na_2CO_3 \rightarrow 2\,REECl_3 + 3\,Na_2SO_4 + 3\,H_2O + 3\,CO_2 \quad (4)$$

Table 4 lists the results assuming a leaching efficiency of 92%, as in Sprecher et al. (2014).

An excess of acid is used to have a good liquid-to-solid ratio, but the unreacted acid, recovered from the residue, is recycled and does not count in the emissions to the environment.

2.2.2.4. Solvent extraction. Solvent extraction (SX) is the most widely used separation technology to separate light REEs from heavy REEs at the industrial scale (El-Nadi, 2017). The modeled process consumes 152 kg of $REECl_3$ concentrate to produce 1 kg of 98.99% Sm_2O_3. As a co-product, 85 kg of other REOs are produced.

Economic allocation was applied for both Nd_2O_3 and Sm_2O_3 and the rest of REOs. Due to the volatility of REEs prices, we employed the price averaging approach recommended for mining and metals (Santero and Hendry, 2016). Industrial SX is carried out in groups of mixer-settlers, called batteries. The process is ineffective if only performed once, as the chemical properties of all the REE are very similar, making separation a challenge (Morais and Ciminelli, 2004). Only with repeated SX steps are the REEs successfully separated from each other. Due to confidentiality reasons, it is not known how many steps exactly are needed to separate $SmCl_3$ from the other REOs. The estimation used in this study is based on a calculation of what is *chemically* needed for a separation of $SmCl_3$ from the other REOs to occur. Generally, most REE extraction operations do not separate $SmCl_3$, since it is a low value REE (Supporting Information, Tables S−3).

Industrial REE SX processes work with modifiers, extractants, and diluents. The SX process modeled uses organic molecules (represented as P204, or $C_{16}H_{35}O_4P$ in this model), often diluted in organic solvents (represented as kerosene in this model). These solutions are able to form stable complexes with the REEs and subsequently are able to be extracted from the feeding solution with a precipitating agent (oxalic acid in this case). Typically, calcination, i.e. heating the oxalates and obtaining a calcine, follows the process of SX. The purpose of calcination is to obtain an oxide through thermal decomposition of REE oxalates to give REE oxides and CO_2. The SX, precipitation, and calcination were all combined in one step to produce 1 kg of Sm_2O_3. This method of combining of steps is analogous to Sprecher et al. (2014).

2.2.2.5. Reduction. Following the SX stage, the production of SmCo alloy differs significantly from that of NdFeB alloy. Rather than electrolysis (as for Nd_2O_3), the Sm_2O_3 is reduced using metallic lanthanum. According to one of the only European companies producing REE alloys, this route is the most popular route for producing samarium metal. The relatively low vapor pressure of samarium at the working conditions causes the samarium to evaporate from the hot mixture of oxides, the samarium vapor leaves the system and the reaction equilibrium is shifted to the right according to the Le Chatelier principle. The reaction is as follows:

$$2\,La + Sm_2O_3 = La_2O_3 + 2\,Sm \quad (5)$$

The lanthanum metal is generally heated with the Sm_2O_3

Table 3
Mass balance of the acid roasting, with basis of 1 kg of $REE_2(SO_4)_3$ in output. Detailed calculations found in Supporting Information − Calculations.

Compound	Mass (kg)
$REE(CO_3)F$	0.53
$REE(PO)_4$	0.30
H_2SO_4	0.37
H_2O	0.07
ThO_2	0.01
$Th(SO_4)_2$	0.15
U_3O_8	0.03
UO_2SO_4	0.05
$REE_2(SO_4)_3$	1.00

Table 4
Mass balance of the conversion of $REE_2(SO_4)_3$ into chlorides with assumed output of 1.00 kg of $REECl_3$. Detailed calculations found in Supporting Information − Calculations.

Compound	Mass (kg)
$REE_2(SO_4)_3$	1.20
HCl	0.82
Na_2CO_3	1.19
H_2CO_3	0.38
Na_2SO_4	2.03
$REECl_3$	1.00

powder at 1330 °C for several hours (Krishnamurthy and Gupta, 2005). The electricity requirement and other LCI parameters were taken from industry surveys in Lee and Wen (2017).

2.2.2.6. Book molding. The casting process starts with broken pieces of book mould of SmCo. The energy consumption was given by an industrial source which uses this process to cast SmCo alloys, reported at 3.6 MJ per kg of material.

2.2.2.7. Coarse milling and jet milling. According to an industrial source, the SmCo production process uses coarse milling along with jet milling since the latter poses a safety risk in transporting very fine particles of SmCo, which are pyrophoric. Coarse milling uses both argon and nitrogen gas. The energy consumption for coarse milling is about 18 MJ per kg of product. For jet milling, the NdFeB data was extrapolated using the temperature profile of SmCo to appropriate the energy consumption for jet milling of SmCo. Yield losses on coarse milling are low, typically less than half of one percent. In this work, loss was assumed as 0.5% as a worst-case scenario.

2.2.2.8. Aligning, pressing, sintering, grinding and slicing. The sintering and heat treatment of SmCo is done in a similar way to NdFeB, with energy and material consumption differing slightly. LCI data was obtained from industrial magnet makers. The total energy consumption for the aligning, pressing, sintering, grinding and slicing processes combined is reported at 15.12 MJ per kg. Losses, occurring at sintering (due to heat treatment) and grinding/slicing, were modeled as 5% and 10% loss respectively.

2.2.2.9. Electroplating. Unlike NdFeB magnets, SmCo magnets do not necessarily require a protective coating (Electron Energy Corporation, 2017; Katter et al., 2001), because of the higher corrosion resistance of SmCo magnets. Nevertheless, customers generally prefer to buy SmCo magnets with a nickel coating as an insurance against wear and tear. In addition, SmCo magnets can be very brittle, the coating reduces risk of chipping. The nickel coating is performed via electroplating.

Electroplating emissions data are based on Moign et al. (2009) which was also used in (Sprecher et al., 2014). $SmCo_5$ magnets were assumed to be electroplated with Ni−Cu−Ni, as indicated by industrial sources. Although both magnets undergo the same electroplating process, the difference in volume of the reference flow leads to different surface area of nickel coating. We assumed 0.068 m^2 of a 15 μm layer for 1 kg of NdFeB magnet, and 0.153 m^2 for the equivalent $SmCo_5$ magnet.

2.3. Sensitivity and uncertainty analysis

A robust uncertainty and sensitivity analysis is imperative for a highly uncertain system such as REE magnet production. In particular when comparing different results from different LCA studies (Heijungs et al. (2010); Björklund (2002)), it is necessary to perform a sensitivity analysis, especially when uncertainty distribution functions are unavailable. There are two reasons why a sensitivity analysis is important: (1) it tells you which parameter affects the model output most; (2) if a parameter is very insensitive, it also almost never contributes to the output uncertainty. In this study, a sensitivity analysis was carried out on 23 parameters. Those with the highest sensitivity percent change (between 2 and 10%) were evaluated in an uncertainty analysis. All parameters surveyed are listed in the Supporting Information, (Tables S−8).

Then the sensitivity ratios (SR) were calculated for both magnet systems. These values are obtained by calculating the variability of the relevant impact category using the formula (6).

$$SR = \frac{\frac{\Delta result}{initial\ result}}{\frac{\Delta parameter}{initial\ parameter}} \quad (6)$$

Since the ±10% variation was used, all SR values higher than 0.2 are assumed to be sensitive.

The subsequent uncertainty analysis explores the three most sensitive parameters identified by the sensitivity analysis. Uncertainty ranges were constructed using literature and expert interviews (see Supporting Information, Table S-5, S-6, and S-7). After defining uncertainty intervals around the key parameters, we employed Monte Carlo simulation to produce a statistical estimate of the final result as well as its standard deviation across 1000 simulation runs.

3. Results

The results of the comparative LCA for the production of $SmCo_5$ and for the production of NdFeB are reported in Table 5. To reiterate, the functional unit is the magnetic performance of 1.0 kg of NdFeB, which is compared with the equivalent 2.04 kg of SmCo.

In terms of overall greenhouse gas (GHG) emissions, we find that SmCo causes emissions of 135 kg of CO_2 equivalent for every 2.04 kg of $SmCo_5$ magnet whereas NdFeB causes emissions of 30 kg.

The human toxicity potential results for NdFeB from 2014 are mostly due to the acid roasting process, whereas the results from this paper are mostly due to the electroplating (Fig. 1). For SmCo, the prevailing contributors to human toxicity potential is the production of cobalt and the acid roasting process. Within the cobalt production process, the highest contributing phase to the global warming potential is the refining of the cobalt metal. For the freshwater aquatic ecotoxicity indicator, the impact for NdFeB is dominated by the nickel used in the coating, which contributes to aquatic pollution. The freshwater aquatic ecotoxicity indicator for SmCo is also highly impacted by the nickel coating as well as the heavy metals emissions in cobalt production. For SmCo, the wastes and losses modeled throughout the post-processing stages for SmCo are also important (Fig. 1).

For both SmCo and NdFeB, the major impacts related to acidification are due to the sulfur dioxide emitted in the production of sulfuric acid for the electroplating. For ozone depletion potential the impacts are related to cobalt production in SmCo and the nickel coating in NdFeB production. For photochemical ozone creation potential, the main impacts are from cobalt production and lanthanum reduction. A significant contributor to the eutrophication potential and photochemical ozone creation is the production of sulfuric acid used in the primary extraction processes for cobalt.

For NdFeB, the photochemical ozone creation potential impacts come mainly from the sulfur dioxide emitted in the production of sulfuric acid for electroplating. For eutrophication potential, the main impact comes from the phosphorous emitted to freshwater in cobalt production for SmCo. For NdFeB the same is true for the nickel production for the electroplating. In Fig. 1, the contribution of all phases of the REE magnet production to environmental impacts are displayed. The mining and production of cobalt represent the highest environmental impact for SmCo, whereas for NdFeB the largest contributor is electroplating.

Sprecher's study showed that 37% of the impacts to the NdFeB magnet were due to the nickel coating (Sprecher et al., 2014). For the entire electroplating process, this updated study shows that this impact is around 65% of the total impacts. If one were to forego the nickel coating for a NdFeB or SmCo and replace it with a thin epoxy resin, the impacts would be reduced. However, the nickel coating is almost always applied due to customer preference. A

Table 5
Impact assessment results from comparative LCA.

CML 2001	SmCo	NdFeB (Sprecher et al., 2014)	NdFeB (this study)
Global Warming Potential (kg-CO_2 equiv)	135.0	25.1	30.2
Acidification Potential (kg-SO_2 equiv)	2.73	0.39	3.37
Eutrophication Potential (kg-Phosphate equiv)	0.21	0.16	0.13
Ozone Depletion (kg-R11 equiv)	1.5×10^{-5}	2.4×10^{-6}	1.08×10^{-6}
Freshwater Ecotoxicity Potential (kg-DCB equiv)	83.8	13.8	92.0
Human Toxicity Potential (kg-DCB equiv)	292	179.8	184
Photochemical Ozone Creation Potential (kg-Ethene equiv)	0.130	0.015	0.139

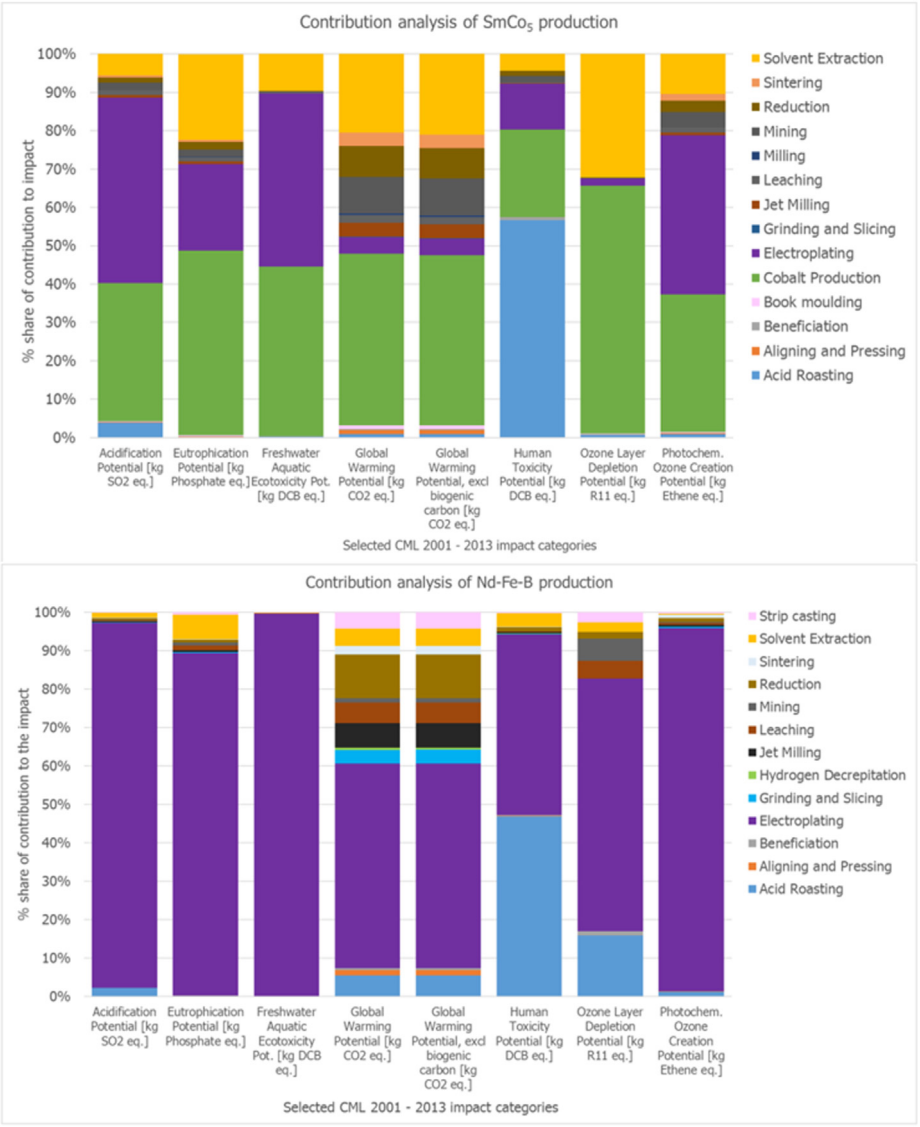

Fig. 1. Results of contribution analysis for production of and SmCo (above) and NdFeB (below).

sensitivity analysis was performed on the surface area of the coating for each magnet to show how greatly the impacts would be affected if the surface layer were reduced or increased. The results of these analyses as well as the others are found in section 3.1.

3.1. Sensitivity analysis

The top three parameters which have the highest sensitivity percent change for both NdFeB and SmCo are: REE content, base metal content, nickel coating layer thickness as shown in Fig. 2. We show the results for GWP, since this was the category with the biggest differences. See Supporting Information, Table S-9 and S-10 for the all sensitivity analysis results for input parameters and impact categories of each system.

The highest SR in the sensitivity analysis is related to the highest contribution to the final life cycle impact assessment results. This one-at-a-time approach sensitivity analysis does not assess the magnitude of the uncertainty of the final results, but is limited to

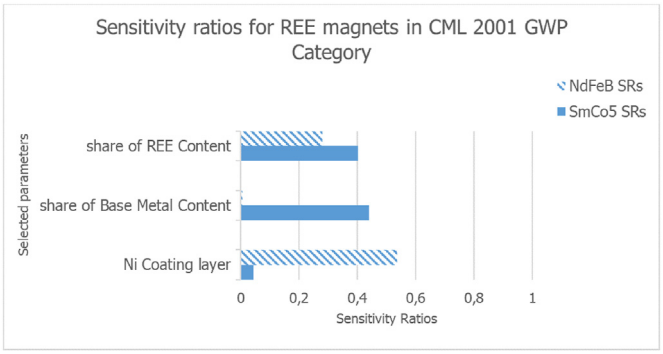

Fig. 2. Sensitivity ratios for Global Warming Potential (GWP, variation 10%).

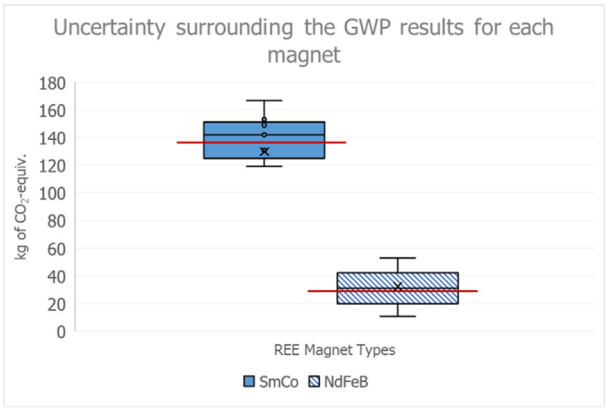

Fig. 3. Boxplot of the Monte Carlo uncertainty results for $SmCo_5$ (blue) and NdFeB (blue lines) magnets, projected GHG emissions for the functional unit. The mean of the output distribution is represented by the X and the median is represented by a solid line within the box. The reference case, or original result scenario (red line), is computed based on the mode of the distribution for each input parameter surveyed. (For interpretation of the references to colour in this figure legend, the reader is referred to the Web version of this article.)

information regarding the sensitivity of the model parameters, by indicating which parameters affect the final result most (Clavreul et al., 2012; Groen, Heijungs, A. M. Bokkers and Boer, 2014).

We make special note of the economic allocation used when modelling the solvent extraction process. Because the price of samarium is much lower than that of neodymium, the impacts of REO production are allocated mostly to neodymium. While in absolute terms it is less significant than the three parameters discussed above, we find that when changing the allocation of Sm_2O_3 from 0.5% to 1% the total GWP results increases of 26%. Conversely, if the allocation coefficient changes for Nd_2O_3 from 34% to 34.5%, the total GWP results do not significantly change. This means that if use of samarium would increase, and subsequently the price of samarium would increase, the environmental impacts of SmCo magnets would also increase significantly, whereas this does not happen for neodymium.

3.2. Uncertainty analysis

Each specific parameter in the model has inherent uncertainty and/or variability. The uncertainty analysis explores the three most sensitive parameters, as identified in section 3.1: REE content, base metal content, nickel coating layer thickness. Standard deviation was based on upper bound and lower bound of values found in literature, augmented with expert judgment (as described in section 2.3 and Supporting Information, Tables S-5, S-6, and S-7).

The results of our 1000 sample Monte Carlo simulation show that the investigated parameters in the NdFeB case are slightly more robust than those of the SmCo case. However, in terms of absolute values, they are quite similar. After performing the Monte Carlo analysis, the GWP results for SmCo will deviate by at most 48%. For NdFeB magnets, the GWP results will deviate by at most 42%. Heijungs (2010) demonstrates that the base case results are equal to that of the median distribution of the GHG emissions. For both NdFeB and SmCo the baseline results of GHG emissions are near the outside fiftieth percentile. The range of uncertainty for each magnet around the coating, REE and alloying content is illustrated in the box plot in Fig. 3.

4. Discussion

The largest contributing process for NdFeB is electroplating, totaling a 65% contribution. Electroplating is also a significant factor in the impact of SmCo. However, in absolute terms, cobalt production is responsible for the largest fraction, 47% (Fig. 1). Cobalt content is an essential factor for SmCo products used in electric vehicle motor applications as it increases its thermal properties. Our results imply that from an environmental point of view, it would be of interest to explore the possibility of Sm_2Co_{17} magnets as an alternative for NdFeB, since they generally contain about 50% less by mass cobalt than $SmCo_5$.

At operational temperatures of high-performance motors, a SmCo magnet will outlast a NdFeB magnet (even when the latter is appropriately doped with dysprosium or terbium). Thus, if one would change the functional unit of this LCA to reflect multiple operation cycles, then a relative reduction could be seen in the environmental impact of SmCo over NdFeB. Nevertheless, since SmCo magnets from electric motors are not reused for multiple vehicle life cycles, such a scenario is not relevant to model.

While there are no individually completed LCA studies to compare the impact assessment results of SmCo magnets, Nordelöf et al. (2019) updated Ecoinvent 3 data for SmCo, reworked with more accurate data about energy use and added a new economic allocation procedure. However, Nordelöf et al. (2019) chose to use the Ecoinvent cobalt dataset instead of the newer one from CDI, which according to the LCA summary report from CDI could lead to about a 30% reduction in GWP results (Cobalt Development Institute, 2016).

When comparing the environmental profiles of samarium metal in Lee and Wen (2017) with this study, we see that Lee and Wen (2017) find that around 106 kg of CO_2-eq is produced for 1 kg of samarium metal, whereas we find 62 kg CO_2-eq. Regarding the impacts related to NdFeB magnets, two recent publications find CO_2-eq values ranging from 89 kg to 41 kg, although direct comparability is difficult due to different deposits, methodologies, and system boundaries (Arshi et al., 2018) (Marx et al., 2018). These differences illustrate how REE life cycle data is still very much incomplete, particularly regarding the upstream processes.

Although the environmental impacts are not necessarily reduced, supply risk could be helped by diversifying the use of different REE materials such as samarium for magnets for electric vehicles motors. Switching from neodymium to samarium would therefore somewhat reduce exposure to REE criticality, although large-scale substitution might cause samarium to become the 'new' bottleneck in the REE balance, rather than neodymium and dysprosium (Binnemans and Jones, 2015). On the other hand, (partial) substitution of REEs with cobalt will not necessarily reduce criticality related issues, as the cobalt supply chain is also problematic on several fronts, including market concentration and labor issues (van den Brink et al., 2020). While SmCo is not better

environmentally, it helps reduce REE criticality by creating a larger pool of diverse supply for REE magnets which can provide a venue for supply chain resilience (Sprecher et al., 2015).

5. Conclusion

We find that $SmCo_5$ does not yield an environmental improvement over NdFeB, with SmCo causing 135 kg of CO_2 emissions, compared to the 30.2 kg for a functionally equivalent amount of NdFeB from our study. Impacts other than CO_2 generally also favor NdFeB, albeit less so. Although these results only hold for the particular combination of data and assumptions used in this study, the magnitude of the difference is significant enough that we are confident of our conclusions. We note that due to economic allocation, and the fact that samarium oxide is much cheaper than neodymium oxide (9 euro/kg and 48 euro/kg, respectively), the relative environmental impact will change, but not the conclusion of this study. If use of samarium would increase, and subsequently the price of samarium would increase, the environmental impacts of SmCo magnets would also increase significantly.

Author statement

Gwendolyn Bailey: performed the Sm–Co LCA and the updated Nd-Fe-B LCA and wrote the manuscript.

Martina Orefice: performed the chemistry calculations and wrote the section on acid roasting and leaching.

Mehmet Recai Onal: assisted with the chemistry calculations.

Enrique Herraiz: assisted with data collection.

Benjamin Sprecher: contributed to the manuscript and performed the Nd-Fe-B LCA for his publication in 2014.

Wim Dewulf: supervised and discussed the results and corrected the manuscript.

Karel Van Acker: supervised and discussed the results and corrected the manuscript.

Declaration of competing interest

The authors declare that they have no known competing financial interests or personal relationships that could have appeared to influence the work reported in this paper.

Acknowledgments

Funding: The research leading to these results has received funding from the European Community's Horizon2020 programme ([H2020/2014–2019]) under Grant Agreement no. 674973 (MSCA-ETN-DEMETER). This publication reflects only the authors' view, exempting the community from any liability. Project website: http://etn-demeter.eu/.

Appendix A. Supplementary data

Supplementary data to this article can be found online at https://doi.org/10.1016/j.jclepro.2020.125294.

References

Arshi, P.S., Vahidi, E., Zhao, F., 2018. Behind the scenes of clean energy: the environmental footprint of rare earth products. ACS Sustain. Chem. Eng. 6 (3), 3311–3320. https://doi.org/10.1021/acssuschemeng.7b03484.

Bailey, G., Joyce, P.J., Schrijvers, D., Schulze, R., Sylvestre, A.M., Sprecher, B., Van Acker, K., 2020. Review and new life cycle assessment for rare earth production from bastnäsite, ion adsorption clays and lateritic monazite. Resour. Conserv. Recycl. 155, 104675.

Binnemans, K., Jones, P.T., 2015. Rare earths and the balance problem. J. Sustain. Metall. 1 (1), 29–38. https://doi.org/10.1007/s40831-014-0005-1.

Binnemans, K., Jones, P.T., Blanpain, B., Van Gerven, T., Yang, Y., Walton, A., Buchert, M., 2013. Recycling of rare earths: a critical review. J. Clean. Prod. 51, 1–22. https://doi.org/10.1016/j.jclepro.2012.12.037.

Björklund, A.E., 2002. Survey of approaches to improve reliability in LCA. Int. J. Life Cycle Assess. 7 (2), 64. https://doi.org/10.1007/bf02978849.

Chen, L., Hopkinson, D., Wang, J., Cockburn, A., Sparkes, M., O'Neill, W., 2015. Reduced dysprosium permanent magnets and their applications in electric vehicle traction motors. IEEE Trans. Magn. 51 (11), 1–4. https://doi.org/10.1109/TMAG.2015.2437373.

Chinese Ministry of Environmental Protection, 2011. Rare earth industry pollution discharge standards. In: Chinese National Standards. China Environmental Science Press, Beijing.

Clavreul, J., Guyonnet, D., Christensen, T.H., 2012. Quantifying uncertainty in LCA-modelling of waste management systems. Waste Manag. 32 (12), 2482–2495. https://doi.org/10.1016/j.wasman.2012.07.008.

El-Nadi, Y.A., 2017. Solvent extraction and its applications on ore processing and recovery of metals: classical approach. Separ. Purif. Rev. 46 (3), 195–215. https://doi.org/10.1080/15422119.2016.1240085.

Electron Energy Corporation (Producer), 2017. About Samarium Cobalt Magnets.

Groen, E., Heijungs, R., Bokkers, E.A.M., Boer, I.J.M., 2014. Sensitivity analysis in life cycle assessment. In: Paper Presented at the 9th International Conference Life Cycle Assessment of Food Conference (LCA Food 2014). San Franciso, USA.

Guinée, J.B., Lindeijer, E., 2002. Handbook on Life Cycle Assessment: Operational Guide to the ISO Standards, vol. 7. Springer Science & Business Media.

Heijungs, R., 2010. Sensitivity coefficients for matrix-based LCA. Int. J. Life Cycle Assess. 15 (5), 511–520. https://doi.org/10.1007/s11367-010-0158-5.

Heijungs, R., Huppes, G., Guinée, J.B., 2010. Life cycle assessment and sustainability analysis of products, materials and technologies. Toward a scientific framework for sustainability life cycle analysis. Polym. Degrad. Stabil. 95 (3), 422–428. https://doi.org/10.1016/j.polymdegradstab.2009.11.010.

Herbst, J.F., Croat, J.J., Pinkerton, F.E., Yelon, W.B., 1984. Relationships between crystal structure and magnetic properties in NdFeB. Phys. Rev. 29 (7), 4176–4178. https://doi.org/10.1103/PhysRevB.29.4176.

IEA, 2011. Radiation Protection and NORM Residue Management in the Production of Rare Earths from Thorium Containing MineralsSafety Reports Series. Retrieved from. http://www-pub.iaea.org/books/IAEABooks/8650/Radiation-Protection-and-NORM-Residue-Management-in-the-Production-of-Rare-Earths-from-Thorium-Containing-Minerals.

Jordens, A., Ping Cheng, Y., Waters, K., 2013. A review of the beneficiation of rare earth element bearing minerals, 41, 97–114. https://doi.org/10.1016/j.mineng.2012.10.017.

Katter, M., Zapf, L., Blank, R., Fernengel, W., Rodewald, W., 2001. Corrosion mechanism of RE-Fe-Co-Cu-Ga-Al-B magnets. In: Paper Presented at the IEEE Transactions on Magnetics.

Krishnamurthy, N., Gupta, C.K., 2005. Extractive Metallurgy of Rare Earths.

Lee, J.C.K., Wen, Z., 2017. Rare earths from mines to metals: comparing environmental impacts from China's main production pathways. J. Ind. Ecol. 21 (5), 1277–1290. https://doi.org/10.1111/jiec.12491.

Li, L.Z., Yang, X., 2014. China's rare earth ore deposits and beneficiation techniques. In: Paper Presented at the European Rare Earth Resource Conference.

Magenti Ljubljana, 2013. In: Ljubljana, M. (Ed.), Permanent Metallic Magnets.

Marx, J., Schreiber, A., Zapp, P., Walachowicz, F., 2018. Comparative life cycle assessment of NdFeB permanent magnet production from different rare earth deposits. ACS Sustain. Chem. Eng. 6 (5), 5858–5867. https://doi.org/10.1021/acssuschemeng.7b04165.

Ministry of Environmental Protection, 2009. The explanation of compiling emission standards of pollutants from rare earths industry.

Moign, A., Vardelle, A., Legoux, J.G., Themelis, N.J., 2009. LCA comparison of electroplating and other thermal spray. Expanding Thermal Spray Perform. New Markets Appl. 1207–1212. https://doi.org/10.1361/cp2009itsc1207.

Morais, C.A., Ciminelli, V., 2004. Process development for the recovery of high-grade lanthanum by solvent extraction. Hydrometallurgy 73 (3–4), 237–244. https://doi.org/10.1016/j.hydromet.2003.10.008.

Navarro, J., Zhao, F., 2014. Life-cycle assessment of the production of rare-earth elements for energy applications: a review. Front. Energy Res. 2, 45. https://doi.org/10.3389/fenrg.2014.00045.

Nordelöf, A., Grunditz, E., Lundmark, S., Tillman, A.-M., Alatalo, M., Thiringer, T., 2019. Life cycle assessment of permanent magnet electric traction motors. Transport. Res. Transport Environ. 67, 263–274.

Norgate, T., Haque, N., 2010. Energy and greenhouse gas impacts of mining and mineral processing operations. J. Clean. Prod. 18 (3), 266–274. https://doi.org/10.1016/j.jclepro.2009.09.020.

Peiró, L.T., Méndez, G.V., 2013. Material and energy requirement for rare earth production. J. Metall. 65 (10), 1327–1340. https://doi.org/10.1007/s11837-013-0719-8.

Sagawa, M., Fujimura, S., Yamamoto, H., Matsuura, Y., 1985. Permanent Magnet Materials Based on the Rare Earth Iron Boron Tetragonal Compounds. https://doi.org/10.1109/TMAG.1984.1063214.

Santero, N., Hendry, J., 2016. Harmonization of LCA methodologies for the metal and mining industry. Int. J. Life Cycle Assess. 21 (11), 1543–1553. https://doi.org/10.1007/s11367-015-1002-4.

Schreiber, A., Marx, J., Zapp, P., Hake, J.-F., Voßenkaul, D., Friedrich, B., 2016. Environmental impacts of rare earth mining and separation based on eudialyte: a new European way. Resources 5 (4), 32. Retrieved from. http://www.mdpi.com/2079-9276/5/4/32.

Shi, F., 2009. Rare Earth Metallurgy. China Metallurgy Industry Press, Beijing.
Sprecher, B., Daigo, I., Murakami, S., Kleijn, R., Vos, M., Kramer, G.J., 2015. Framework for resilience in material supply chains, with a case study from the 2010 rare Earth crisis. Environ. Sci. Technol. 49 (11), 6740–6750. https://doi.org/10.1021/acs.est.5b00206.
Sprecher, B., Xiao, Y., Walton, A., Speight, J., Harris, R., Kleijn, R., Kramer, G.J., 2014. Life cycle inventory of the production of rare earths and the subsequent production of NdFeB rare earth permanent magnets. Environ. Sci. Technol. 48 (7), 3951–3958. https://doi.org/10.1021/es404596q.
Strnat, K., Hoffer, G., Olson, J., Ostertag, W., Becker, J.J., 1967. Family New Cobalt-Base Permanent Magnet Mater. 38 (3), 1001–1002. https://doi.org/10.1063/1.1709459.
Tharumarajah, R., Koltun, P., 2011. Cradle to gate assessment of environmental impact of rare earth metals. In: Paper Presented at the Proceedings of the 7th Australian Conference on Life Cycle Assessment. Melbourne, Australia.
The Cobalt Development Institute, 2016. The Environmental Performance of Refined Cobalt: Life Cycle Inventory and Life Cycle Assessment of Refined Cobalt - Summary Report. Retrieved from Environmental Resources Management Limited.
Vahidi, Ehsan, Navarro, Julio, Zhao, Fu, 2016. “An initial life cycle assessment of rare earth oxides production from ion-adsorption clays.”. Resources Conservation and Recycling 1–11. https://doi.org/10.1016/j.resconrec.2016.05.006.
Vahidi, E., Zhao, F., 2017. Environmental life cycle assessment on the separation of rare earth oxides through solvent extraction. J. Environ. Manag. https://doi.org/10.1016/j.jenvman.2017.07.076.
van den Brink, S., Kleijn, R., Sprecher, B., Tukker, A., 2020. Identifying supply risks by mapping the cobalt supply chain. Resour. Conserv. Recycl. 156, 104743.
Wernet, G., Bauer, C., Steubing, B., Reinhard, J., Moreno-Ruiz, E., Weidema, B., 2016. The ecoinvent database version 3 (part I): overview and methodology. Int. J. Life Cycle Assess. 21 (9), 1218–1230. https://doi.org/10.1007/s11367-016-1087-8.